A Novel Enzyme Complex of Orotate Phosphoribosyltransferase and Orotidine 5′-Monophosphate Decarboxylase in Human Malaria Parasite *Plasmodium falciparum*: Physical Association, Kinetics, and Inhibition Characterization[†,‡]

Sudaratana R. Krungkrai,[§,||,⊥] Brian J. DelFraino,[#] Jeffrey A. Smiley,[#] Phisit Prapunwattana,[§] Toshihide Mitamura,[||] Toshihiro Horii,[||] and Jerapan Krungkrai*[,§]

Department of Biochemistry, Faculty of Medicine, Chulalongkorn University, Rama 4 Road, Bangkok 10330, Thailand, Department of Molecular Protozoology, Research Institute for Microbial Diseases, Osaka University, 3-1 Yamadaoka, Suita, Osaka 565-0871, Japan, and Department of Chemistry, Youngstown State University, Youngstown, Ohio 44555

Received July 22, 2004; Revised Manuscript Received November 17, 2004

ABSTRACT: Human malaria parasite, *Plasmodium falciparum*, can only synthesize pyrimidine nucleotides using the de novo pathway, whereas mammalian cells obtain pyrimidine nucleotides from both the de novo and salvage pathways. The parasite's orotate phosphoribosyltransferase (*Pf*OPRT) and orotidine 5′-monophosphate decarboxylase (*Pf*OMPDC) of the de novo pyrimidine pathway are attractive targets for antimalarial drug development. Previously, we have reported that the two enzymes in *P. falciparum* exist as a multienzyme complex containing two subunits each of 33-kDa *Pf*OPRT and 38-kDa *Pf*OMPDC. In this report, the gene encoding *Pf*OPRT has been cloned and expressed in *Escherichia coli*. An open reading frame of *Pf*OMPDC gene was identified in the malaria genome database, and *Pf*OMPDC was cloned from *P. falciparum* cDNA, functionally expressed in *E. coli*, purified, and characterized. The protein sequence has <20% identity with human OMPDC and four microbial OMPDC for which crystal structures are known. Recombinant *Pf*OMPDC was catalytically active in a dimeric form. Both recombinant *Pf*OPRT and *Pf*OMPDC monofunctional enzymes were kinetically different from the native multienzyme complex purified from *P. falciparum*. Oligomerization of *Pf*OPRT and *Pf*OMPDC cross-linked by dimethyl suberimidate indicated that they were tightly associated as the heterotetrameric 140-kDa complex, $(Pf\text{OPRT})_2(Pf\text{OMPDC})_2$. Kinetic analysis of the *Pf*OPRT−*Pf*OMPDC associated complex was similar to that of the native *P. falciparum* enzymes and was different from that of the bifunctional human enzymes. Interestingly, a nanomolar inhibitor of the yeast OMPDC, 6-thiocarboxamido-uridine 5′-monophosphate, was about 5 orders of magnitude less effective on the *Pf*OMPDC than on the yeast enzyme. Our results support that the malaria parasite has unique structural and functional properties, sharing characteristics of the monofunctional pyrimidine-metabolizing enzymes in prokaryotes and bifunctional complexes in eukaryotes.

Malaria is a major cause of morbidity and mortality in developing countries. More than a third of the world's population live in malaria-endemic areas, and 1 billion people are estimated to carry malaria parasites at any one time (*1*). In Africa alone, there are an estimated 300−500 million cases of malaria and up to 3 million people die from the disease each year (*2*). *Plasmodium falciparum* is the causative agent of the most lethal and severe form of human malaria. Chemotherapy of malaria is available but is complicated by both drug toxicity and widespread resistance to most of the currently available antimalarial drugs (*3*, *4*). The need for more efficacious and less toxic agents, particularly rational drugs that exploit metabolic pathways and targets unique to the parasite, is therefore acute (*5*, *6*).

Plasmodia species are dependent on de novo synthesis of pyrimidine nucleotides (Scheme 1) because they lack salvage enzymes (*7*−*10*), whereas the mammalian host cells obtain pyrimidines from both de novo and salvage pathways (*11*, *12*). Inhibition of de novo pyrimidine synthesis by specific inhibitors, e.g., orotate analogues (*13*, *14*) and atovaquone (*14*, *15*), thus leads to dramatic reduction in cellular pyrimidine pools and eventual failure of the parasite to survive. Such inhibitors are found to have strong antimalarial activity for *P. falciparum* grown in vitro and *Plasmodium berghei* propagated in mice (*13*, *14*).

The final two steps of uridine 5′-monophosphate (UMP)[1] synthesis require the addition of ribose 5-phosphate from

[†] S.R.K. is a Japan Society for the Promotion of Science RONPAKU Fellow. This work was partially supported by the Thailand Research Fund (BRG4580020, to J.K.); Grant-in-Aid for Scientific Research (A) (13357002) and Grant-in-Aid for Scientific Research on Priority Areas (13226058) (to T.H.) from the Ministry of Education, Science, Sports, Culture and Technology of Japan; and National Institutes of Health, AREA program (Grant GM63504-01, to J.A.S.).

[‡] The nucleotide sequence reported in this paper has been deposited in the DDBJ Data Bank with accession number AB074431.

* Corresponding author. Tel: (662)-2564482. Fax: (662)-2524963. E-mail: fmedjkk@md2.md.chula.ac.th.

[§] Chulalongkorn University.

[||] Osaka University.

[⊥] Present address: Department of Medical Science, Faculty of Science, Rangsit University, Patumthani 12000, Thailand.

[#] Youngstown State University.

10.1021/bi048439h CCC: $30.25
Published on Web 01/14/2005

Scheme 1: Six Sequential Steps of De Novo Pyrimidine Biosynthesis in *P. falciparum*

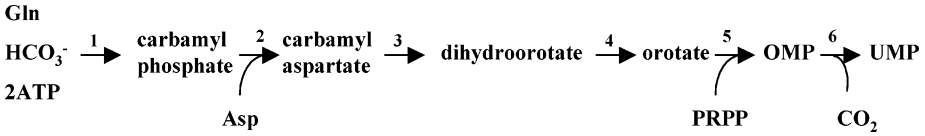

5-phosphoribosyl-1-pyrophosphate (PRPP) to orotate by orotate phosphoribosyltransferase (EC 2.4.2.10, OPRT) to form orotidine 5′-monophosphate (OMP) and the subsequent decarboxylation of OMP to form UMP by OMP decarboxylase (EC 4.1.1.23, OMPDC). These enzymes are encoded by two separate genes in most prokaryotes, whereas their sequences in most multicellular organisms are joined into a single gene, resulting in the bifunctional UMP synthase (UMPS) (*16*, *17*).

Our recent studies have shown that OPRT and OMPDC exist as a multienzyme complex in *P. falciparum* and *P. berghei* (*18*, *19*). Potent inhibitors of malarial OPRT and OMPDC, Pyrazofurin and its 5′-monophosphate metabolite, were found to be effective antimalarial agents (*14*, *20*, *21*). The gene encoding *P. falciparum* OPRT (*Pf*OPRT) has been identified, cloned, and functionally expressed in *Escherichia coli* (*21*).

In this study, we report cloning, expression, and characterization of the gene encoding OMPDC (*Pf*OMPDC) from cDNA of *P. falciparum* in *E. coli*. We demonstrate that the recombinant *Pf*OPRT obtained from the previous study (*21*) and the purified recombinant *Pf*OMPDC can form a tightly associated multienzyme complex in vitro. Physical interaction and kinetic properties of the *Pf*OPRT−*Pf*OMPDC complex from the combination of the two recombinant sources are comparable to those of the native heterotetrameric (*Pf*OPRT)$_2$-(*Pf*OMPDC)$_2$ complex existing in *P. falciparum*. In contrast, these properties are different from those of the bifunctional human enzymes.

EXPERIMENTAL PROCEDURES

Materials. Yeast OPRT and OMPDC enzymes were purchased from Sigma. Reagents for cell culture, protein purification and enzymatic assays were purchased from standard sources (listed where necessary). Reagents were the highest quality commercially available and were used without further purification, except OMP and PRPP, which were purified using a high-performance liquid chromatographic (HPLC) method as described (*22*). The HPLC system was purchased from Spectra-Physics. The fast protein liquid chromatographic (FPLC) system was purchased from Amersham Biosciences. 6-Thiocarboxamido-UMP (6-CSNH$_2$-UMP) was synthesized according to the procedures of Ueda et al. (*23*). Solutions of 6-CSNH$_2$UMP were quantified using the extinction coefficient of $\epsilon_{270} = 11\,300\ M^{-1}\ cm^{-1}$ (*23*). 5-Fluoro-UMP (5-FUMP) was prepared from 5-fluoroorotate (5 mmol) by a reaction of yeast OPRT and yeast OMPDC (10 units each) and then purified by HPLC as described (*22*).

Parasites and Preparation of Parasite Cell-Free Crude Extract. The asexual stage of *P. falciparum* strain T9 was cultivated by the candle jar method of Trager and Jensen (*24*) with some modifications as described (*19*). The parasites were isolated from human red cells and then lysed in the presence of protease inhibitors cocktail to prevent high protease activities in the parasites as described (*8*, *19*). The cell-free crude extract was obtained after centrifugation of the lysate at 27 000*g* for 60 min.

Purification of Native OPRT and OMPDC Enzymes from P. falciparum. The native OPRT and OMPDC enzymes were purified from the freshly prepared cell-free crude extract by three sequential chromatographic steps on Mono Q anion exchange FPLC, UMP-agarose affinity (Sigma), and Superose 12 gel filtration FPLC columns, as described previously (*19*) with the following buffer: 50 mM Hepes, pH 7.4, 5 mM DTT, and 20% glycerol. The purity of the enzymes was assessed by SDS−PAGE. The purified enzymes were stored as aliquots in the presence of 5 mM DTT and 20% glycerol at −80 °C.

Preparation of P. falciparum DNA, RNA, and cDNA. Genomic DNA and total RNA were isolated from *P. falciparum* as described (*21*). cDNA was synthesized from total RNA using reverse transcription-polymerase chain reaction (RT-PCR) as described (*21*).

Cloning, Expression, and Purification of Recombinant PfOPRT from P. falciparum cDNA. The open reading frame (846 bp) encoding OPRT was identified on chromosome 5 in the *P. falciparum* genome database (*25*). The *Pf*OPRT was cloned, expressed, and purified as described (*21*) with some modifications by using a different expression vector and host *E. coli*. Briefly, the coding region for the *Pf*OPRT was amplified from the cDNA of *P. falciparum* by PCR and ligated into a pQE30Xa vector (Qiagen). The *Pf*OPRT was expressed in *E. coli* SG13009 (Qiagen) in the presence of 1 mM isopropyl β-D-thiogalactopyranoside (IPTG) at 18 °C for 18 h. The recombinant protein was purified using Ni^{2+}−NTA−agarose affinity chromatography (Qiagen). The His$_6$-tag was removed from the protein by using factor Xa (Qiagen). The protein was further purified by a Superose 12 gel filtration FPLC column equilibrated with a buffer of 50 mM Tris-HCl, pH 8.0, 300 mM NaCl, 5 mM DTT, and 1 mM PMSF. The purified enzyme was eluted with a retention time corresponding to a molecular mass of 66 kDa, which is its dimeric form. SDS−PAGE analysis of the recombinant *Pf*OPRT corresponded to a 33-kDa monomer.

Cloning, Expression, and Purification of Recombinant PfOMPDC from P. falciparum cDNA. The gene homologue encoding *Pf*OMPDC was identified as a single open reading frame (969 bp) on chromosome 10 in the *P. falciparum*

[1] Abbreviations: 6-azaUMP, 6-aza-uridine 5′-monophosphate; 6-CONH$_2$UMP, 6-carboxamidouridine 5′-monophosphate; DMS, 3,3′-dimethylsuberimidate; DTT, 1,4-dithiothreitol; FPLC, fast protein liquid chromatography; 5-FUMP, 5-fluorouridine 5′-monophosphate; HPLC, high-performance liquid chromatography; Hepes, *N*-2-hydroxyethylpiperazine-N′-4-ethanesulfonic acid; IPTG, isopropyl β-D-thiogalactopyranoside; Ni^{2+}−NTA, nickel−nitrilotriacetic acid; OPRT, orotate phosphoribosyltransferse; OMP, orotidine 5′-monophosphate; OMPDC, OMP decarboxylase; PMSF, phenylmethylsulfonyl fluoride; *Pf*OPRT, *P. falciparum* OPRT; *Pf*OMPDC, *P. falciparum* OMPDC; PRPP, 5-phosphoribosyl-1-pyrophosphate; SDS−PAGE, sodium dodecyl sulfate−polyacrylamide gel electrophoresis; 6-CSNH$_2$UMP, 6-thiocarboxamido-uridine 5′-monophosphate; UMP, uridine 5′-monophosphate; UMPS, UMP synthase.

genome database (*25*). RT-PCR was used to amplify *Pf*OMPDC cDNA using total RNA as the template.

The forward primer was 5′ CG**GGATCC**ATGGGTTTTAAGGTAAAATTA 3′ and the reverse primer was 5′ CC**ATCGAT**TTACGATTCCATATTTTGCTTTAA 3′ which introduce *BamH* I and *Cla* I restriction sites respectively (shown in bold). The PCR conditions were similar to those described for *Pf*OPRT (*21*). The PCR products were purified and ligated into a pTrcHis-TOPO plasmid (Invitrogen). The *Pf*OMPDC sequence was determined in both directions by the dideoxy chain termination method using an automated Applied Biosystems model 377 sequencer. Competent *E. coli* TOP10 (Invitrogen) cells were transformed with the recombinant plasmid, induced with 1 mM IPTG at 18 °C for 18 h, harvested, and stored as cell paste at −80 °C. The recombinant *Pf*OMPDC from the cell paste was purified using a Ni^{2+}−NTA−agarose affinity column. The recombinant protein was then subjected to His_6-tag removal using enterokinase (Invitrogen). The protein was further purified by the Superose 12 gel filtration FPLC.

Enzymatic Assays. OPRT and OMPDC activities were measured according to previously described spectrophotometric methods (*26*−*28*). The OPRT enzymatic reaction was monitored by a decrease in absorbance of orotate, whereas the OMPDC reaction was monitored by a decrease in absorbance of OMP and also by an appearance of UMP in an HPLC chromatogram, as essentially described (*19*, *22*).

Enzyme Kinetics and Inhibition Studies. For all kinetic analyses for both OPRT and OMPDC, the purified native and recombinant enzymes, after Superose 12 gel filtration FPLC column chromatography (>97% pure as observed by SDS−PAGE), were used at concentrations of 15−30 nM in 1.0 mL reaction assays, and their kinetics was measured in three to five different preparations. The K_m and V_{max} values were determined by measurement of initial velocities in triplicate with at least five substrate concentrations. The k_{cat} values were calculated as described (*29*). The catalytic efficiency (k_{cat}/K_m) for OPRT and OMPDC and of the 1:1 mixture of OPRT and OMPDC was also calculated.

Where inhibition studies were performed on the mixture of OPRT and OMPDC and on each enzyme separately, three different concentrations of inhibitors were tested for initial velocity measurements. Kinetic data of the initial velocities and inhibitions were fitted to an equation for competitive inhibitors (eq 1) using the method of Cleland (*30*).

$$v = \frac{V_{max}[S]}{[S] + K_m\left(1 + \frac{[I]}{K_i}\right)} \quad (1)$$

Oligomerization and Chemical Cross-Linking of PfOPRT and PfOMPDC. To demonstrate whether the *Pf*OPRT and the *Pf*OMPDC form an oligomeric multienzyme complex, chemical cross-linking of either *Pf*OPRT or *Pf*OMPDC were performed using the bifunctional reagent 3,3′-dimethylsuberimidate (DMS) as described (*21*, *31*). The cross-linking reaction was initiated by the addition of DMS (20 μg) to the pure recombinant *Pf*OPRT and/or *Pf*OMPDC (10 μg each), and the reaction incubated at 25 °C for various time intervals. The reaction was then quenched by the addition of 1 M glycine to a concentration of 0.1 M. The cross-linked species were analyzed by SDS−PAGE. The molecular masses of the cross-linked species were also analyzed with a Superose 12 gel filtration FPLC column.

Oligomeric *Pf*OPRT and *Pf*OMPDC enzymes in their native forms were formed by incubating the two enzymes (0.5 mg/mL each) with either 0.25 mM orotate and 0.25 mM PRPP or 0.5 mM UMP in a buffer containing 50 mM Tris-HCl, pH 8.0, 300 mM NaCl, 5 mM $MgCl_2$, and 2.5 mM DTT at 37 °C for 10 min. The oligomeric forms were then analyzed and purified by a Superose 12 gel filtration FPLC column. Both OPRT and OMPDC activities were then measured.

Miscellaneous Methods. Protein concentrations were determined by the Bradford assay (*32*) using bovine serum albumin as standard. Concentrations of pure *Pf*OPRT and *Pf*OMPDC were measured using ϵ_{280} values of 21 760 and 33 280 M^{-1} cm^{-1}, respectively. The ϵ values for both enzymes (monomeric forms) were calculated according to Edelhoch (*33*).

SDS−PAGE was performed on a Bio-Rad gel apparatus with polyacrylamide gels of 7%−12% in the buffer system of Laemmli (*34*). The gels were stained with Coomassie brilliant blue R and visualized by Bio-Rad molecular analyst PC software image analysis.

The Superose 12 gel filtration FPLC column was equilibrated with the buffer described before and calibrated with molecular mass markers: blue dextran 2000 (2000 kDa, V_0), thyroglobulin (670 kDa), immunoglobulin (158 kDa), bovine serum albumin (66 kDa), ovalbumin (44 kDa), myoglobin (17 kDa), and vitamin B_{12} (1.35 kDa, V_t).

Homology search was performed using the BLAST program (*35*). Pairwise and multiple sequence alignments of *Pf*OMPDC with other organisms were performed using the CLUSTALW program (*36*). Hydrophobicity of the *Pf*OMPDC was determined by the DNASIS program (Hitachi) and the Kyte−Doolittle plot as described (*37*). Western blot analysis was performed to confirm the authenticity of the His_6-tagged recombinant *Pf*OPRT and *Pf*OMPDC proteins as described (*38*).

RESULTS AND DISCUSSION

OPRT and OMPDC activities in human and multicellular organisms are conferred by 51-kDa bifunctional UMPS protein (*11*, *16*, *27*, *39*, *40*), whereas the enzymes appear to have two forms in lower eukaryotes: monofunctional forms, such as in *Saccharomyces cerevisae* (*26*), or a bifunctional form, as is seen in *Trypanosoma cruzi* and *Leishmania mexicana* (*41*, *42*). In bacteria, they are monofunctional enzymes (*43*). An exception for these enzymes has been found in the malaria parasites, where they exist as a multienzyme complex, $(PfOPRT)_2(PfOMPDC)_2$ (*18*,*19*). Recent efforts with cDNA microarray analysis of the *P. falciparum* genes show that the *Pf*OPRT and *Pf*OMPDC genes are actively expressed in the asexual erythrocytic stage (*44*). The *Pf*OPRT gene and the recombinant protein have been characterized (*21*). Production of recombinant *Pf*OPRT and *Pf*OMPDC can provide the appropriate quantities of the homogeneous enzymes for characterizations of physical, kinetic, inhibitory effect, and stability properties of individual monofunctional enzyme. The tightly associated complex of

the two enzymes can then be compared to those properties of the multienzyme complex purified from *P. falciparum* grown in vitro.

Purification and Characterization of Native OPRT and OMPDC Multienzyme Complex from P. falciparum. Activities of OPRT and OMPDC in the cell-free crude extracts of *P. falciparum* were ~20−25 nmol min^{-1} mg^{-1} protein. The use of Hepes buffer (pH 7.4), 5 mM DTT, 20% glycerol, and the protease inhibitors cocktail stabilized the enzyme activities during purification. Following the crude extracts, the OPRT and OMPDC activities were copurified by Mono Q anion exchange, UMP−agarose affinity, and Superose 12 gel filtration columns with the maximal activity of each enzyme found together. The enzymes were purified with specific activities of ~9−12 μmol min^{-1} mg^{-1} protein and ~420−450-fold with overall yield of ~35−40%. This purification strategy provided ~0.25 mg of purified enzymes from 2 L of *P. falciparum* culture having ~2−3 times more active enzymes (k_{cat} values in the range of 10.8−24.6 s^{-1}) than our previous report (*19*). In vivo concentrations of the enzymes were accurately calculated by using the equation described (*27*) and the parasite's intracellular volume of 1.35 mL/g dry weight (*45*). The cellular concentrations of the enzymes in *P. falciparum* were 60 ± 5 nM ($n = 6$), about 2.5-fold more than those of the human UMPS (*27*). The bacteria, such as *E. coli*, and yeast have increased concentrations of the separate monofunctional enzymes by about 10−50-fold, and the stability of both enzymes is decreased (*27*). The large differences of the in vivo protein concentrations would reflect greater lability of the monofunctional enzymes than the bifunctional human enzyme (*27*) or *P. falciparum* multienzyme complex in this study.

At the Superose 12 FPLC purification step, the active fractions containing OPRT and OMPDC were eluted in a single peak with a molecular mass of 140 kDa. SDS−PAGE of the purified OPRT and OMPDC resulted in the monomeric forms with the molecular mass of 33 and 38 kDa, respectively. These results indicate the occurrence of the 140-kDa $(OPRT)_2(OMPDC)_2$ complex. The purified complex was stable (>90% activity remaining) for at least 6 months at −20 or −80 °C in 50 mM Hepes buffer, pH 7.4, 300 mM NaCl, 5 mM DTT, and 20% glycerol. Under the same condition but at 4 °C, the enzyme activities were decreased to 50% after 4-week storage. When the enzymes were stored in the absence of DTT and glycerol, their activities were gradually decreased to 50% after 1 week at 4 °C (half-life ~ 7 days). Repeated applications of the stored enzymes (at 4 °C and 2 weeks) on a Superose 12 FPLC column gave low enzyme activities, eluting with retention times corresponding to their monomeric forms (33 kDa for OPRT and 38 kDa for OMPDC). These labile properties would explain the previous report on the discrete activities of OPRT and OMPDC in *P. falciparum* cytosol observed after one-step purification on a Cibracon blue affinity column (*46*).

Purification and Characterization of Monofunctional PfOPRT. The deduced protein sequence of *Pf*OPRT (281 amino acids) has high similarity (percent similarity indicated in parentheses) to bacterial enzymes, such as *E. coli* (60%) and *Salmonella typhimurium* (56%). It shows low similarity to protozoan *T. cruzi* (30%) and to human OPRT domain of UMPS enzyme (28%). Catalytic residues and the consensus sequences for orotate and PRPP substrate bindings of the two known crystal structures of *S. typhimurium* (*47*, *48*) and *E. coli* (*49*) OPRTs are well-conserved in the malarial protein sequence (*21*). Since there is a common metabolic intermediate, OMP, involved in the OPRT and OMPDC reactions (Scheme 1), the protein sequences of both *P. falciparum* enzymes were aligned pairwise. Both enzymes were markedly different in the active site loops and had only 16% identity, which is quite similar to comparisons of both enzymes in yeast and human. These data indicate that OPRT and OMPDC may not share an evolutionary relationship, in contrast to previous suggestions (*42*, *50*). This is consistent with the dissimilarity of the tertiary structures between OPRT and OMPDC.

The cDNA encoding *Pf*OPRT was directly cloned into the vector pQE30Xa and expressed in the *E. coli* SG13009 cells. This strategy yielded ~4 mg of pure *Pf*OPRT from 1 L of cell culture, which was 4-fold higher than that expressed in the expression vector pET-15b and the *E. coli* strain BL21-(DE3) cells containing the RIG plasmid (*21*, *51*). The *Pf*OPRT was a homodimer of two 33-kDa monomers as $(PfOPRT)_2$, with a 67-kDa molecular mass on a Superose 12 gel filtration FPLC column and a 33-kDa molecular mass by SDS−PAGE (data not shown), which is consistent with the dimeric form in the crystal structures (*47*−*49*). The k_{cat} of the recombinant *Pf*OPRT was 4.2 s^{-1}, ~1.5-fold more active than the enzyme obtained in our previous preparation (*21*). The monofunctional *Pf*OPRT enzyme was stable in the presence of 5 mM DTT and 20% glycerol, i.e., >90% activity remained for at least 3 months at −20 and −80 °C. When the enzyme was stored in the absence of DTT and glycerol, the activity decreased to 50% after overnight storage at 4 °C (half-life ~ 1 day).

Cloning and Identification of PfOMPDC Homologue. The cDNA encoding *Pf*OMPDC was cloned in the pTrcHis-TOPO vector and the nucleotide sequence was then verified. The protein sequence of the *Pf*OMPDC consists of 323 amino acids, with 6 Arg (~2 mol %), 17 Asp (~5 mol %), 33 Lys (~10 mol %), and 40 Asn (~12 mol %), a molecular mass of 37 822 Da, and an isoelectric point of 7.6 (Figure 1). The *Pf*OMPDC protein sequence is more similar to the protozoan (*T. cruzi*, *L. mexicana*) (*42*) and to some bacterial counterparts (*Thermus thermophilus*, *Mycobacterium smegmatis*) (*42*) than to the OMPDC domain of human UMPS (*52*). The *Pf*OMPDC sequence has 33, 32, 31, 27 and 14% identity to *T. cruzi*, *L. mexicana*, *T. thermophilus*, *M. smegmatis*, and human enzymes, respectively. However, the sequence identities of the four known crystal structures of OMPDCs, i.e., *Bacillus subtilis* (*53*), *E. coli* (*54*), *Methanobacterium thermoautotrophicum* (*55*), and *S. cerevisae* (*56*), are <20% to the malarial enzyme (Figure 1). Similar to *Pf*OPRT (*21*), *Pf*OMPDC contains an extension of 32 amino acids from its N-terminus (Met1 to Phe32) and a unique insertion of 12 amino acids from Arg72 to Phe83, displaying a hydrophobic index of +1.0. *Pf*OMPDC is one of the longest OMPDC sequences to date, including the *Neurospora crassa* OMPDC (*57*). The average protein for all 82 species contains 270 amino acids (*57*). Similar extensions and insertions of different amino acid sequences are found in malarial proteins, but their origin and function remain unknown (*21*, *58*−*60*).

In comparison with the OMPDC crystal structures from *B. subtilis*, *E. coli*, *M. thermoautotrophicum*, and *S. cerevisae*

FIGURE 1: Multiple sequence alignments of *P. falciparum* OMPDC with four known crystal structures. Numbers in parentheses are accession numbers: *B. subtilis* (AA21273), *E. coli* (NP_415797), *M. thermoautotrophicum* (NP_275272), and *S. cerevisae* (AAA34824.1). Bold letters indicated the most conserved active site residues; italic letters are similar amino acids. Three active site loops (I, II, III) of *Pf*OMPDC are identified and marked by upper lines and underlines.

(Figure 1), 10 active site residues are well-conserved in the *P. falciparum* sequence, i.e., Asp68, Lys102, Asp136, Lys138, Asp141, Ile142, Thr145, Ser207, Gly293, and Arg294. The alignment gives an uncertain comparison in the portion of the sequence around the conserved active site glutamine, Gln215 (yeast). Alignment of the *P. falciparum* sequence with the *M. thermoautotrophicum* one alone would result in the alignment of *P. falciparum* Gln269 with *M. thermoautotrophicum* Gln185, the known active site residue. However, comparison with the *E. coli* sequence results in the alignment of *P. falciparum* Gln269 with the *E. coli* residue Gln194, which is not in the active site, and suggests that the *P. falciparum* equivalent of the *E. coli* active site residue Gln201 is Asn279. The latter of these two possibilities seems to fit best with the four sequences taken together; apparently this portion of the active site in the four structures is somewhat different in the *P. falciparum* enzyme. Although the active site residue Gln215 (yeast) is conserved among all structures and virtually all sequences, its replacement in the yeast enzyme with alanine results in very little impairment of decarboxylase activity (*61*).

In addition, many residues involved in TIM barrel formation are most similar in the five organism sequences, shown as italic letters in Figure 1. All crystal structures are composed of two identical subunits, each containing one active site located at the top of the TIM barrel, near the subunit−subunit interface, and showing both the N- and C-termini extending side-by side on one surface of the protein. It is postulated that the N-terminal of *Pf*OMPDC could bind to the N-terminal of the *Pf*OPRT, leading to heterotetrameric $(PfOPRT)_2(PfOMPDC)_2$ complex formation. However, this remains to be studied.

Expression, Purification, and Characterization of Monofunctional PfOMPDC. The construct pTrcHis-TOPO vector with *Pf*OMPDC sequence was then expressed in *E. coli* TOP10. The recombinant *Pf*OMPDC protein was purified to apparent homogeneity using a Ni^{2+}−NTA affinity column. The His_6-tag of the *Pf*OMPDC was removed, and the protein

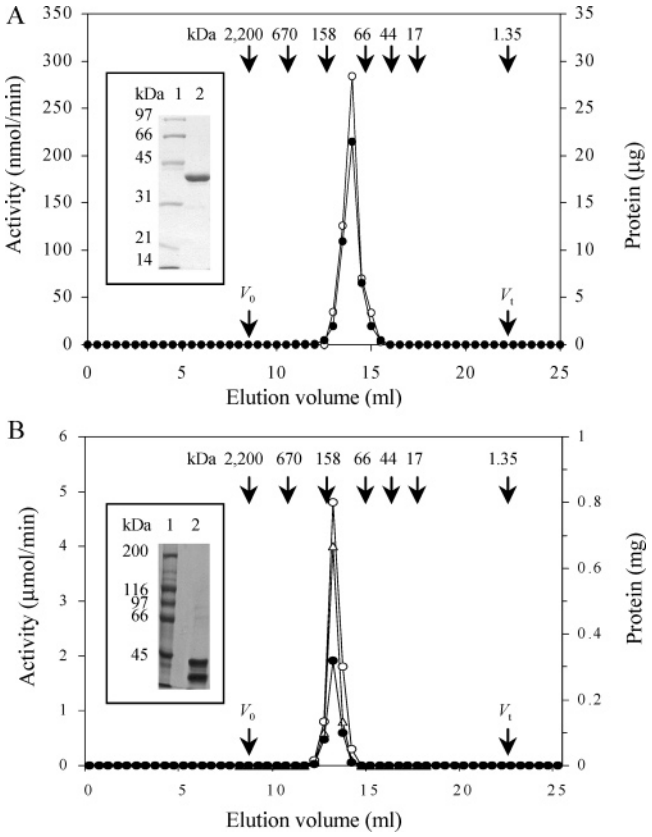

FIGURE 2: (A) Dimeric form of the recombinant *Pf*OMPDC enzyme. A chromatogram for the Superose 12 gel filtration FPLC column of the purified *Pf*OMPDC is illustrated. The peaks of enzyme activity per 0.5-mL fraction (○) and protein concentration (●) are eluted together at a molecular mass of 76 kDa. Molecular mass markers (Amersham Biosciences) provided in kDa, void volume (V_0), and total eluting volume (V_t) are indicated with arrows. SDS−PAGE on a 12% polyacrylamide gel of the purified *Pf*OMPDC (10 μg) shows a homogeneous preparation at a molecular mass of 38 kDa (inset, lane 2). Low molecular mass markers (Bio-Rad) are given in kDa (inset, lane 1). (B) Heterotetrameric formation of *Pf*OPRT and *Pf*OMPDC enzymes. A chromatogram for the Superose 12 gel filtration FPLC column of the 1:1 mixture of *Pf*OPRT and *Pf*OMPDC dimeric forms is shown. In the 0.5-mL fraction, peaks of both enzyme activities (△, *Pf*OPRT; ○, *Pf*OMPDC) and protein concentration (●) are eluted symmetrically at a molecular mass of 140 kDa. Molecular mass markers provided in kDa, void volume (V_0) and total eluting volume (V_t) are indicated with arrows. SDS−PAGE on a 10% polyacrylamide gel of the active fractions at 12.5 mL (∼140 kDa complex) (30 μg) shows two major bands at molecular masses of 33 and 38 kDa, corresponding to their monomeric sizes (inset, lane 2). High molecular mass markers (Bio-Rad) are given in kDa (inset, lane 1).

was further purified by a Superose 12 gel filtration FPLC column. The *Pf*OMPDC enzyme activity was eluted in a single peak with a molecular mass of 76 ± 4 kDa (n = 8) (Figure 2A). By SDS−PAGE analysis, the monomeric form of the *Pf*OMPDC had a molecular mass of 38 ± 3 kDa (n = 8) (Figure 2A, inset), corresponding to the predicted value for the protein sequence. The purity of the protein, assessed by 12% gel of SDS−PAGE and image analyses, was more than 97%. The purified recombinant enzyme had a specific activity of ∼8−10 μmol min^{-1} mg^{-1} protein, 220-fold purification, and 30% yield, and up to 3 mg of pure protein was obtained from 1 L of cell culture. Recently, Menz et al. (*62*) have used pMICO vector for *Pf*OMPDC expression, and a much lower protein yield was obtained. This limits further characterization of the protein. Our recombinant *Pf*OMPDC is catalytically active in its dimeric form, as found for the bacterial and yeast proteins in the crystal structures (*53*−*56*). The active enzyme was stable (>90% activity remaining) in the presence of 5 mM DTT and 20% glycerol for at least 4 months at −20 and −80 °C. When the enzyme was stored in the absence of DTT and glycerol, its activity was decreased to 50% after 3 days at 4 °C (half-life ∼ 3 days), and its aggregation was observed at a protein concentration of more than 2 mg/mL.

Heterotetrameric Formation of Recombinant PfOPRT and PfOMPDC. Using oligomerization studies of a mixture of the recombinant *Pf*OPRT and *Pf*OMPDC in a stoichiometric ratio of 1:1, the association complex was analyzed by a Superose 12 gel filtration FPLC column after incubating the enzymes with the substrates orotate and PRPP at 300 mM NaCl, Tris-HCl, pH 8.0, for 10 min at 37 °C. Both enzyme activities were coeluted as a single, symmetrical peak at a retention time corresponding to a molecular mass of 140 ± 6 kDa (n = 6) (Figure 2B). There were no enzyme activities remaining at their dimeric positions and also no activities in fractions corresponding to molecular masses higher than 140 kDa, indicating the essentially complete heterotetrameric complex formation between $(OPRT)_2$ and $(OMPDC)_2$. The oligomerization of both enzymes were also performed by incubating the enzymes in the presence or absence of the product UMP; similar results to the enzymes incubated with the substrates were obtained (data not shown). These suggest that the complex would be stabilized by substrate, product, and salt. The fractions containing both *Pf*OPRT and *Pf*OMPDC were pooled and then analyzed by SDS−PAGE, whereupon two bands were observed at their monomeric forms of 33 and 38 kDa for both enzymes (Figure 2B, inset). The purified fractions were subsequently analyzed for their kinetic properties, providing a comparison to their monofunctional forms. Stability of the purified heterotetrameric enzymes was achieved by the addition of 5 mM DTT and 20% glycerol. In the absence of both stabilizers, both enzyme activities were gradually declined ∼60% after 1 week at 4 °C (half-life ∼ 6 days), similar to their stability properties found in the native complex from *P. falciparum*.

To confirm the complex formation, a second approach using chemical cross-linking of either *Pf*OPRT or *Pf*OMPDC was performed by incubating the enzymes with DMS in a ratio of 1:2 protein to cross-linker at 25 °C for various time intervals, followed by SDS−PAGE analysis. The cross-linked product of *Pf*OMPDC was observed to a greater extent as the dimeric form with a molecular mass of 75 ± 5 kDa (n = 6) within 5-min incubation (data not shown). The cross-linked product of recombinant *Pf*OPRT was a dimer with a molecular mass of 67 kDa, as demonstrated previously (*21*). Neither recombinant enzyme (10 μg) formed a tetramer when incubating with increasing amounts of DMS up to 100 μg after 60 min and overnight at 25 °C. When the cross-linked dimeric products of *Pf*OPRT and *Pf*OMPDC were mixed and further incubated with DMS for various times, more than 70% of the dimers converted to the tetramers within 5 min and no hexameric form was detected (data not shown).

When a mixture of *Pf*OPRT and *Pf*OMPDC (each 10 μg) was incubated with 40 μg of DMS, there was significant formation of tetramer at 10-min incubation, as shown in Figure 3. At 30 min, more than 70% of the proteins were cross-linked as tetrameric form. There was little hexameric

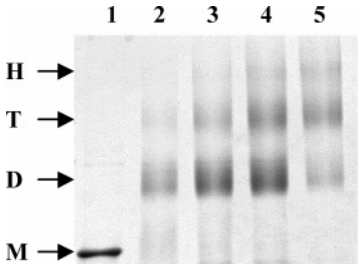

FIGURE 3: SDS−PAGE analysis of oligomeric formation between *Pf*OPRT and *Pf*OMPDC cross-linked with dimethyl suberimidate (DMS). SDS−PAGE on a 7% polyacrylamide gel shows time-course of cross-linking between *Pf*OPRT and *Pf*OMPDC (each 10 μg) and DMS (40 μg) at 0 min (lane 1), 5 min (lane 2), 10 min (lane 3), 15 min (lane 4), 30 min (lane 5). The letters M, D, T, and H indicate positions of monomeric, dimeric, tetrameric, and hexameric forms. The apparent monomer, dimer, tetramer, and hexamer have log molecular mass of 4.58, 4.85, 5.15, and 5.33, respectively.

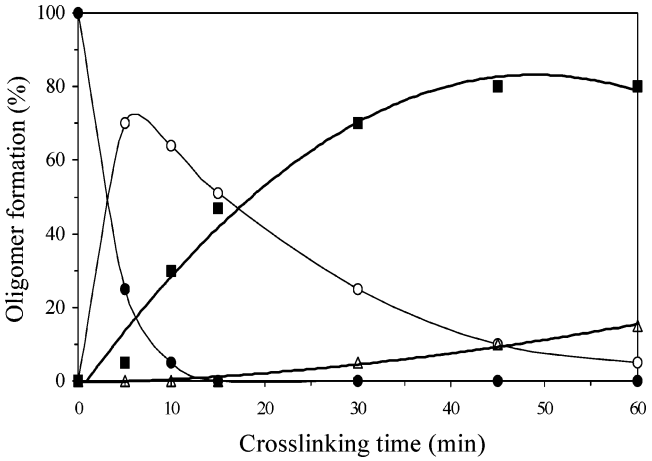

FIGURE 4: Kinetics of cross-linking between the *Pf*OPRT and *Pf*OMPDC by dimethyl suberimidate. The experimental details are described in Figure 3. The time dependence of the percentage of each size of oligomers as indicated by the ratio of its band density to the total density of all detected bands is illustrated. The symbols used are as follows: monomer (●), dimer (○), tetramer (■), and hexamer (△).

form and no octameric form after 45−120-min incubation. The cross-linked products gave a broad banding pattern during SDS−PAGE (Figure 3) and also image analyses, in particular due to the major tetrameric form. However, the linear relationship between the log of molecular mass, calculated assuming that these oligomers were all multiples of the monomer and dimer, and the electrophoretical mobility confirmed the assignment. The molecular masses of the cross-linked oligomers were also determined by a Superose12 gel filtration FPLC column. The tetramer had a molecular mass of 140 ± 12 kDa ($n = 6$), corresponding to the size of the native multienzyme complex from *P. falciparum*. Kinetic analyses of cross-linking of both associated enzymes are shown in Figure 4, indicate that the time-dependent oligomerization of each enzyme corresponded to that expected for sequential cross-linking of monomer → dimer → tetramer. Taken together, these results demonstrated that the two pyrimidine enzymes, $(Pf\text{OPRT})_2$ and $(Pf\text{OMPDC})_2$, form a major oligomeric complex with a heterotetrameric structure (Scheme 2).

Kinetic Properties of Monofunctional PfOMPDC and PfOPRT, Their Heterotetrameric Form, and the Native

Scheme 2: A Proposed Model for Multienzyme $(OPRT)_2(OMPDC)_2$ Complex Formation of *P. falciparum* OPRT and OMPDC[a]

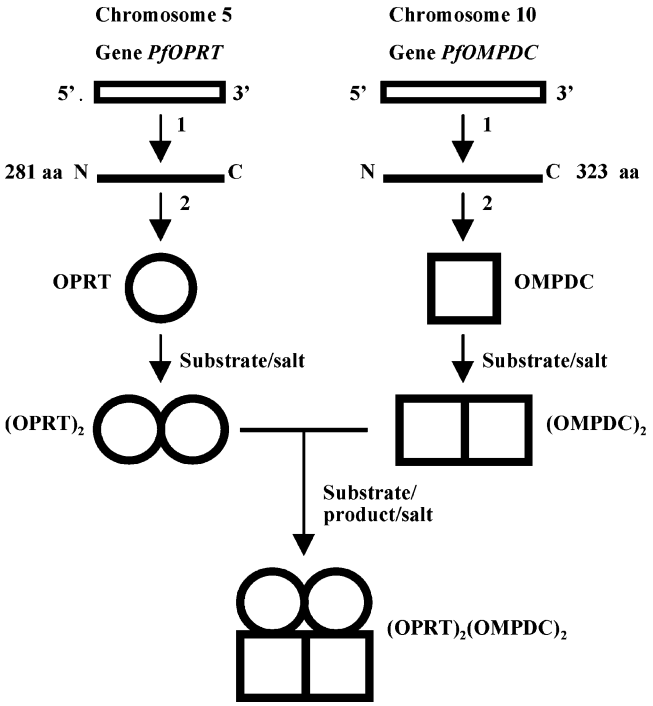

[a] The genes encoding OPRT and OMPDC are distinctive: when the recombinant proteins are produced separately, the individual enzymes form homodimers. Both enzymes are functioning with optimal kinetic constants in a tightly associated heterotetrameric form.

OPRT−OMPDC Multienzyme Complex. The monofunctional *Pf*OMPDC activity had a pH optimum range from 6.0 to 8.0, similar to other OMPDCs (*16*, *26*, *63*, *64*), with a k_{cat} of 7.5 s^{-1}, and a K_m of 13.4 ± 1.2 μM ($n = 6$). In addition, the catalytic reaction of *Pf*OMPDC was Mg^{2+}- or Zn^{2+}-independent and found to be irreversible. At the concentration range of 0.25−1.0 mM, neither Mg^{2+} nor Zn^{2+} had any effect on the enzyme activity; similar properties are demonstrated in the yeast enzyme (*65*).

Kinetic parameters of the monofunctional *Pf*OPRT and *Pf*OMPDC, their heterotetrameric form isolated from the 1:1 mixture by a Superose 12 gel filtration FPLC column, and the native OPRT and OMPDC multienzyme complex purified from *P. falciparum* are shown in Tables 1 and 2. These kinetic values are compared to kinetic parameters reported for human monofunctional OPRT and OMPDC and bifunctional UMPS expressed in the baculovirus system (*27*, *66*). The monofunctional *Pf*OPRT showed 2-fold lower catalytic efficiency (k_{cat}/K_m) than the monofunctional human OPRT, but their k_{cat} values were quite similar. However, the monofunctional *Pf*OMPDC had 80-fold lower catalytic efficiency than the monofunctional human OMPDC; most of this effect was due to a higher K_m of *Pf*OMPDC for OMP. In previous studies of mouse UMPS, the K_m of the monofunctional OMPDC expressed in yeast is 3-fold higher than the value obtained for the bifunctional mouse UMPS (*39*), but these values are quite similar between the recombinant human OMPDC domain and UMPS (*27*). Comparing the kinetic parameters in three different forms of the two enzymes, the K_m values for both enzymes in the multienzyme complex and in the enzyme mixture are ∼3−4-fold lower than these values in the monofunctional forms, and the k_{cat}

Table 1: Enzyme Kinetic Constants of OPRT in Monofunctional Recombinant *Pf*OPRT, a 1:1 Mixture of Recombinant *Pf*OPRT and *Pf*OMPDC, Native *P. falciparum* Multienzyme Complex, and Monofunctional OPRT Domain and Bifunctional Human UMPS Enzyme

	$K_m^{orotate}$ (μM)	K_m^{PRPP} (μM)	k_{cat}[a] (s^{-1})	k_{cat}/K_m[a] ($M^{-1}\ s^{-1}$)
P. falciparum				
monofunctional *Pf*OPRT	18.2 ± 0.9	28.6 ± 1.3	4.2	2.3×10^5
*Pf*OPRT and *Pf*OMPDC mixture	4.5 ± 0.7	16.4 ± 1.0	6.0	1.3×10^6
multienzyme complex	5.6 ± 0.8	11.3 ± 1.0	10.8	1.9×10^6
Human[b]				
monofunctional OPRT domain	7.1 ± 0.3		2.9	4.1×10^5
bifunctional enzyme	2.1 ± 0.1		4.0	1.9×10^6

[a] Calculated values were taken from the $K_m^{orotate}$ measurement for comparison with the human enzymes. [b] Data for the isolated OPRT domain and bifunctional UMPS of human enzymes were calculated from Yablonski et al. (*27*).

Table 2: Enzyme Kinetic Constants of OMPDC in Monofunctional Recombinant *Pf*OMPDC, a 1:1 Mixture of Recombinant *Pf*OPRT and *Pf*OMPDC, Native *P. falciparum* Multienzyme Complex, and Monofunctional OMPDC Domain and Bifunctional Human UMPS

	K_m^{OMP} (μM)	k_{cat} (s^{-1})	k_{cat}/K_m ($M^{-1}\ s^{-1}$)
P. falciparum			
monofunctional *Pf*OMPDC	13.4 ± 1.2	7.5	5.6×10^5
*Pf*OPRT and *Pf*OMPDC mixture	5.6 ± 0.8	18.2	3.3×10^6
multienzyme complex	3.2 ± 0.4	24.6	7.7×10^6
Human[a]			
monofunctional OMPDC domain	0.29 ± 0.02	13.0	4.5×10^7
bifunctional enzyme	0.23 ± 0.01	16.0	7.0×10^7

[a] Data for the isolated OMPDC domain and bifunctional UMPS of human enzymes were calculated from Yablonski et al. (*27*).

values are higher. Catalytic efficiencies of the multienzyme complex and the enzyme mixture are ~6−14-fold greater than those values for the monofunctional forms. However, the K_m values of OMP in these three forms of *Pf*OMPDC are 10-fold less than those reported in the human and yeast enzymes. These results indicate that the tight association between the two enzymes would favor efficient catalysis by lowering K_m and increasing k_{cat}.

Characterization of Enzyme Inhibition. Lines of evidence for inhibition studies of product UMP and three analogues on two different forms of the *Pf*OMPDC are provided and compared to previous observations. Table 3 shows K_i values observed for the inhibitors of monofunctional *Pf*OMPDC, monofunctional yeast enzyme, native *P. falciparum* OPRT and OMPDC multienzyme complex, and bifunctional human UMPS. In all cases, inhibition was fitted to eq 1 and appeared to be competitive. Previously, we have shown that 5-fluoroorotate is an effective alternative substrate for the *Pf*OPRT and exhibits strong antimalarial activity with 50% inhibitory effect of approximately 6 nM on *P. falciparum* grown in vitro and shows potent in vivo antimalarial effect on *P. berghei* in mice (*13*, *21*). This compound would serve as a subversive substrate for the malarial enzymes. Such type of compounds may be useful in antimalarial drug design targeting malarial OPRT and OMPDC enzyme complex. Moreover, uracil and 5-fluorouracil were not substrates for the *Pf*OPRT and exhibited weak inhibition (*21*). The property

Table 3: K_i Values (M) for OMPDC Inhibitors of Monofunctional *Pf*OMPDC, Yeast Monofunctional Enzyme, Native *P. falciparum* Multienzyme Complex, and Human Bifunctional UMPS

	P. falciparum			
inhibitor	monofunctional	multienzyme	yeast[a]	human[b]
6-azaUMP	1.0×10^{-6}	1.4×10^{-7}	6.4×10^{-8}	5.0×10^{-9}
5-FUMP	1.2×10^{-6}	6.7×10^{-7}		
6-$CSNH_2$UMP	1.7×10^{-4}	2.4×10^{-4}	3.5×10^{-9}	
6-$CONH_2$UMP			6.0×10^{-4}	
UMP	2.5×10^{-4}	1.2×10^{-4}	2.0×10^{-4}	2.4×10^{-5}

[a] Data of the monofunctional yeast OMPDC were taken from Miller et al. (*69*) and Miller and Wolfenden (*70*). [b] Data of the bifunctional human UMPS were taken from Livingstone and Jones (*16*).

is similar to *S. typhimurium* OPRT (*47*), in contrast to the human OPRT domain of UMPS, in which 5-fluorouracil serves as a substrate and finally converts to 5-fluorodeoxyUMP, a potent anticancer drug (*67*). 5-FUMP and 6-azaUMP were found to be potent inhibitors of *Pf*OMPDC at submicromolar levels, with even lower K_i values in the multienzyme complex. These values are about 15- and 30-fold less than those for the yeast and human enzymes, respectively.

The binding affinities of the UMP analogues to either monofunctional *Pf*OMPDC or multienzyme complex increases in a series: UMP < 6-$CSNH_2$UMP < OMP < 5-FUMP < 6-azaUMP. The binding order is similar to those of the human OMPDC domain of UMPS (*16*, *68*) and yeast OMPDC (*69*, *70*), except for 6-$CSNH_2$UMP, which is a very potent inhibitor ($K_i = 3.5 \times 10^{-9}$ M) of yeast OMPDC (*65*, *69*) yet only a weak inhibitor of *Pf*OMPDC with K_i values in the range of $1.7-2.4 \times 10^{-4}$ M. Using commercially available yeast OMPDC with the inhibitor, the obtained K_i was nearly in the nanomolar range, as in the published literature. There have been no reports investigating this inhibitor binding to active site residues of OMPDCs in the known crystals. If 6-$CSNH_2$UMP binds to OMPDC with the uracil ring of the nucleotide situated in the same orientation as the inhibitors in the crystal structures, then the difference in K_i for 6-$CSNH_2$UMP between the yeast and *P. falciparum* enzymes would be a result of different contacts between the thiocarboxamide group and the respective Lys-Asp-Lys-Asp charged networks at the active sites. If 6-$CSNH_2$UMP binds to OMPDC with the uracil ring of the nucleotide situated in the opposite orientation as the inhibitors in the crystal structures, as has been proposed for the binding of OMP versus these inhibitors (*71*), then the difference in K_i for 6-$CSNH_2$UMP between the yeast and *P. falciparum* enzymes would be a result of different contacts between the thiocarboxamide group and the respective portions of the active site near the conserved glutamine—Gln215 of the yeast enzyme—and an unconfirmed residue in the *P. falciparum* sequence (possibly Asn279). Regardless, the active sites of *P. falciparum* and human OMPDCs appear quite different and susceptible to variable degrees of inhibition, an inviting prospect for drug intervention.

CONCLUSIONS

The last two enzymes of the de novo pyrimidine biosynthetic pathway in *P. falciparum* exist as a $(OPRT)_2$-$(OMPDC)_2$ 140-kDa heterotetrameric complex, an organi-

zation that is possibly exploitable for the design of new antimalarial drugs. This proposal, illustrated in Scheme 2, is firmly supported by the lines of evidence as follows: (1) the tightly associated complex of the two recombinant enzymes by native oligomerization induced by substrate, product, and salt, and by dimethyl suberimidate chemical cross-linking; (2) kinetic parameters favoring the multienzyme complex prepared from *P. falciparum* and from mixtures of the recombinant enzymes, comparable to the bifunctional human enzymes; (3) inhibition constants of known OMPDC inhibitors confirming stronger affinity to the multienzyme complex than to the monofunctional enzyme, similar to the human enzymes; and (4) less stability of the monofunctional enzymes than the multienzyme complex and the human enzymes.

ACKNOWLEDGMENT

We thank S. Kudan and N. Wutipraditkul for their technical assistance. We also thank N. M. Q. Palacpac and S. Aoki for helpful discussion in this work.

REFERENCES

1. Guerin, P. J., Olliaro, P., Nosten, F., Druilhe, P., Laxminarayan, R., Blinka, F., Kilama, W. L., Ford, N., and White, N. J. (2002) Malaria: Current status of control, diagnosis, treatment, and a proposed agenda for research and development, *Lancet Infect. Dis. 2*, 564−573.
2. Marsh, K. (1998) Malaria disaster in Africa, *Lancet 352*, 924−925.
3. Attaran, A., Barnes, K. I., Curtis, C., d'Alessandro, U., Fanello, C. I., Galinski, M. R., Kokwaro, G., Looareesuwan, S., Makanga, M., Mutabingwa, T. K., Talisuna, A., Trape, J. F., and Watkins, W. M. (2004) WHO, the Global Fund, and medical malpractice in malaria treatment, *Lancet 363*, 237−240.
4. White, N. J. (2004) Antimalarial drug resistance, *J. Clin. Invest. 113*, 1084−1092.
5. Ginsburg, H. (2002) Malaria metabolic maps: http://huji.ac.il/malaria/.
6. Ridley, R. G. (2002) Medical need, scientific opportunity and the drive for antimalarial drugs, *Nature 415*, 686−693.
7. Gero, A. M., and O'Sullivan, W. J. (1990) Purines and pyrimidines in malarial parasites, *Blood Cells 16*, 467−484.
8. Krungkrai, J., Cerami, A., and Henderson, G. B. (1990) Pyrimidine biosynthesis in parasitic protozoa: Purification of a monofunctional dihydroorotase from *Plasmodium berghei* and *Crithidia fasciculata*, *Biochemistry 29*, 6270−6275.
9. Krungkrai, J., Cerami, A., and Henderson, G. B. (1991) Purification and characterization of dihydroorotate dehydrogenase from the rodent malaria parasite *Plasmodium berghei*, *Biochemistry 30*, 1934−1939.
10. Krungkrai, J. (1993) Dihydroorotase and dihydroorotate dehydrogenase as a target for antimalarial drugs, *Drugs Future 18*, 441−450.
11. Jones, M. E. (1980) Pyrimidine nucleotide biosynthesis in animals: Genes, enzymes, and regulation of UMP biosynthesis, *Annu. Rev. Biochem. 49*, 253−279.
12. Weber, G. (1983) Biochemical strategy of cancer cells and the design of chemotherapy, *Cancer Res. 43*, 466−492.
13. Krungkrai, J., Krungkrai, S. R., and Phakanont, K. (1992) Antimalarial activity of orotate analogs that inhibit dihydroorotase and dihydroorotate dehydrogenase, *Biochem. Pharmacol. 43*, 1295−1301.
14. Seymour, K. K., Lyons, S. D., Phillips, L., Rieckmann, K. H., and Christopherson, R. I. (1994) Cytotoxic effects of inhibitors of *de novo* pyrimidine biosynthesis upon *Plasmodium falciparum*, *Biochemistry 33*, 5268−5274.
15. Krungkrai, J. (1995) Purification, characterization and localization of mitochondrial dihydroorotate dehydrogenase in *Plasmodium falciparum*, human malaria parasite, *Biochim. Biophys. Acta 1243*, 351−360.
16. Livingstone, L. R., and Jones, M. E. (1987) The purification and preliminary characterization of UMP synthase from human placenta, *J. Biol. Chem. 262*, 15726−15733.
17. Suchi, M., Mizuno, H., Kawai, Y., Tsuboi, T., Sumi, S., Okajima, K., Hodgson, M. E., Ogawa, H., and Wada, Y. (1997) Molecular cloning of human UMP synthase gene and characterization of point mutations in two hereditary orotic aciduria families, *Am. J. Hum. Genet. 60*, 525−539.
18. Krungkrai, J., Prapunwatana, P., Wichitkul, C., Reungprapavut, S., Krungkrai, S. R., and Horii, T. (2003) Molecular biology and biochemistry of malarial parasite pyrimidine biosynthetic pathway, *Southeast Asian J. Trop. Med. Public Health 34 Suppl 3*, 32−43.
19. Krungkrai, S. R., Prpapunwattana, P., Horii, T., and Krungkrai. J. (2004) Orotate phosphoribosyltransferase and orotidine 5′-monophosphate decarboxylase exists as multienzyme complex in malaria parasite *Plasmodium falciparum*, *Biochem. Biophys. Res. Commun. 318*, 1012−1018.
20. Scott, H. V., Gero, A. M., and O'Sullivan, W. J. (1986) In vitro inhibition of *Plasmodium falciparum* by Pyrazofurin, an inhibitor of pyrimidine biosynthesis de novo, *Mol. Biochem. Parasitol. 18*, 3−15.
21. Krungkrai, S. R., Aoki, S., Palacpac, N. M. Q., Sato, D., Mitamura, M., Krungkrai, J., and Horii, T. (2004) Human malaria parasite orotate phosphoribosyltransferase: Functional expression, characterization of kinetic reaction mechanism and inhibition profile, *Mol. Biochem. Parasitol. 134*, 245−255.
22. Krungkrai, J., Wutipraditkul, N., Prapunwattana, P., Krungkrai, S. R., and Rochanakij, S. (2001) A nonradioactive high-performance liquid chromatographic microassay for uridine 5′-monophosphate synthase, orotate phosphoribosyltransferase, and orotidine 5′-monophosphate decarboxylase, *Anal. Biochem. 299*, 162−168.
23. Ueda, T., Yamamoto, M., Yamane, A., Imazawa, M., and Inoue, H. (1978) Conversion of uridine nucleotides to the 6-cyano derivatives: Synthesis of orotidylic acid. *J. Carbohydr. Nucleosides Nucleotides 5*, 361−371.
24. Trager, W., and Jensen, J. B. (1976) Human malaria parasites in continuous culture, *Science 193*, 673−675.
25. Gardner, M. J., Hall, N., Fung, E., White, O., Berriman, M., Hyman, R. W., Carlton, J. M., Pain, A., Nelson, K. E., Bowman, S., Paulsen, I. T., James, K., Eisen, J. A., Rutherford, K., Salzberg, S. L., Craig, A., Kyes, S., Chan, M., Nene, V., Shallom, S. J., Suh, B., Peterson, J., Angiuoli, S., Pertea, M., Allen, J., Selengut, J., Haft, D., Mather, M. W., Vaidya, A. B., Martin, D. M. A., Fairlamb, A. H., Fraunholz, M. J., Roos, D. S., Ralph, S. A., McFadden, G. I., Cummings, L. M., Subramanian, G. M., Mungall, C., Venter, J. C., Carucci, D. J., Hoffman, S. L., Newbold, C., Davis, R. W., Fraser, C. M., and Barrell, B. (2002) Genome sequence of the human malaria parasite *Plasmodium falciparum*, *Nature 419*, 498−511.
26. Umezu, K., Amaya, T., Yoshimoto, A., and Tomita, K. (1971) Purification and properties of orotidine 5′-phosphate pyrophosphorylase and orotidine 5′-phosphate decarboxylase from Bakers' yeast, *J. Biochem. 70*, 249−262.
27. Yablonski, M. J., Pasek, D. A., Han, B., Jones, M. E., and Traut, T. W. (1996) Intrinsic activity and stability of bifunctional human UMP synthase and its two separate catalytic domains, orotate phosphoribosyltransferase and orotidine 5′-phosphate decarboxylase, *J. Biol. Chem. 271*, 10704−10708.
28. Poulsen, P., Jensen, K. F., Hansen, P. V., Carlsson, P., and Lundberg, L. G. (1983) Nucleotide sequence of the *Escherichia coli pyrE* gene and of the DNA in front of the protein-coding region, *Eur. J. Biochem. 135*, 223−229.
29. Segel, I. H. (1975) *Enzyme kinetics: Behavior and analysis of rapid equilibrium and steady-state enzyme systems*, Wiley, New York.
30. Cleland, W. W. (1979) Statistical analysis of enzyme kinetic data, *Methods Enzymol. 63*, 103−138.
31. Lee, L., Kelly, R. E., Pastra-Landis, S. C., and Evans, D. R. (1985) Oligomeric structure of the multifunctional protein CAD that initiates pyrimidine biosynthesis in mammalian cells, *Proc. Natl. Acad. Sci. U.S.A. 82*, 6802−6806.
32. Bradford, M. M. (1976) A rapid and sensitive method for the quantitation of microgram quantities of protein utilising the principle of protein−dye binding, *Anal. Biochem. 72*, 248−254.
33. Edelhoch, H. (1967) Spectroscopic determination of tryptophan and tyrosine proteins, *Biochemistry 6*, 1948−1954.

34. Laemmli, U. K. (1970) Cleavage of structural proteins during assembly of the head of bacteriophage T4, *Nature 227*, 680−685.
35. Altschul, S. F., Madden, T. L., Schaffer, A. A., Zang, J., Zang, Z., Miller, W., and Lipman, D. J. (1997) Gapped BLAST and PSI−BLAST: A new generation of protein database search programs, *Nucleic Acids Res. 25*, 3389−3402.
36. Thompson, J. D., Higgins, D. G., and Gibson, T. J. (1994) CLUSTALW: Improving the sensitivity of progressive multiple sequence alignment through sequence weighting, position-specific gap penalties and weight matrix choice, *Nucleic Acids Res. 22*, 4673−4680.
37. Kyte, J., and Doolittle, R. F. (1982) A simple method for displaying the hydropathic character of a protein, *J. Mol. Biol. 157*, 105−132.
38. Towbin, H., Staeheli, T., and Gordon, J. (1979) Electrophoretic transfer of proteins from polyacrylamide gels to nitrocellulose sheets: Procedure and some applications, *Proc. Natl. Acad. Sci. U.S.A. 76*, 4350−4354.
39. Langdon, S. D., and Jones, M. E. (1987) Study of the kinetic and physical properties of the orotidine-5′-monophosphate decarboxylase domain from mouse UMP synthase produced in *Saccharomyces cerevisiae*, *J. Biol. Chem. 262*, 13359−13365.
40. Floyd, E. E., and Jones, M. E. (1985) Isolation and characterization of the orotidine 5′-monophosphate decarboxylase domain of the multifunctional protein uridine 5′-monophosphate synthase, *J. Biol. Chem. 260*, 9443−9451.
41. Gao, G., Nara, T., Shimada, J. N., and Aoki, T. (1999) Novel organization and sequences of five genes encoding all six enzymes for de novo pyrimidine biosynthesis in *Trypanosoma cruzi*, *J. Mol. Biol. 285*, 149−161.
42. Nara, T., Hshimoto, T., and Aoki, T. (2000) Evolutionary implications of the mosaic pyrimidine-biosynthetic pathway in eukaryotes, *Gene 257*, 209−222.
43. Grogan, D. W., and Gunsalus, R. P. (1993) *Sulfolobus acidocaldarius* synthesizes UMP via a standard de novo pathway: Results of a biochemical−genetic study, *J. Bacteriol. 175*, 1500−1507.
44. Bozdech, Z., Llinas, M., Pulliam, B. L., Wong, E. D., Zhu, J., and DeRisi, J. L. (2003) The transcriptome of the intraerythrocytic developmental cycle of *Plasmodium falciparum*, *PLOS Biol. 1*, 85−100.
45. Krugliak, M., Zhang, J., and Ginsburg, H. (2002) Intraerythrocytic *Plasmodium falciparum* utilizes only a fraction of the amino acids derived from the digestion of host cell cytosol for the biosynthesis of its protein, *Mol. Biochem. Parasitol. 119*, 249−256.
46. Rathod, P. K., and Reyes, P. (1983) Orotidylate-metabolizing enzymes of the human malarial parasite, *Plasmodium falciparum*, differ from host cell enzymes, *J. Biol. Chem. 258*, 2852−2855.
47. Scapin, G., Grubmeyer, C., and Sacchettini, J. C. (1994) Crystal structure of orotate phosphoribosyltransferase, *Biochemistry 33*, 1287−1294.
48. Scapin, G., Ozturk, D. H., Grubmeyer, C., and Sacchettini, J. C. (1995) The crystal structure of the orotate phosphoribosyltransferase complexed with orotate and α-D-5-phosphoribosyl-1-pyrophosphate, *Biochemistry 34*, 10744−10754.
49. Henriksen, A., Aghajari, N., Jensen, K. F., and Gajhede, M. (1996) A flexible loop at the dimer interface is a part of the active site of the adjacent monomer of *Escherichia coli* orotate phosphoribosyltransferase, *Biochemistry 35*, 3803−3809.
50. Shostak, K., and Jones, M. E. (1992) Orotidylate decarboxylase: Insights into the catalytic mechanism from substrate specificity studies, *Biochemistry 31*, 12155−12161.
51. Baca, M. A., and Hol, W. G. J. (2000) Overcoming codon bias: A method for the high-level overexpression of *Plasmodium* and other AT-rich parasite genes in *Escherichia coli*, *Int. J. Parasitol. 30*, 113−118.
52. Suttle, D. P., Bugg, B. Y. Winkler, J. K., and Kanalas, J. J. (1988) Molecular cloning and nucleotide sequence for the complete coding regions of human UMP synthase. *Proc. Natl. Acad. Sci. U.S.A. 85*, 1754−1758.
53. Appleby, T. C., Kinsland, C., Begley, T. P., and Ealick, S. E. (2000) The crystal structure and mechanism of orotidine 5′-monophosphate decarboxylase, *Proc. Natl. Acad. Sci. U.S.A. 97*, 2005−2010.
54. Harris, P., Poulsen, J.-C. N., Jensen, K. F., and Larsen, S. (2000) Structural basis for the catalytic mechanism of a proficient enzyme: Orotidine 5′-monophosphate decarboxylase, *Biochemistry 39*, 4217−4224.
55. Wu, N., Mo, Y., Gao, J., and Pai, E. F. (2000) Electrostatic stress in catalysis: Structure and mechanism of the enzyme orotidine monophosphate decarboxylase, *Proc. Natl. Acad. Sci. U.S.A. 97*, 2017−2022.
56. Miller, B. G., Hassell, A. M., Wolfenden, R., Milburn, M. V., and Short, S. A. (2000) Anatomy of a proficient enzyme: The structure of orotidine 5′-monophosphate decarboxylase in the presence and absence of a potential transition state analog, *Proc. Natl. Acad. Sci. U.S.A. 97*, 2011−2016.
57. Traut, T. W., and Jones, M. E. (1996) Uracil metabolism-UMP synthesis from orotic acid or uridine and conversion of uracil to β-alanine: Enzymes and cDNAs, *Prog. Nucleic Acids Res. Mol. Biol. 53*, 1−78.
58. Gilberger, T.-W., Schirmer, R. H., Walter, R. D., and Muller, S. (2000) Deletion of the parasite-specific insertions and mutation of the catalytic triad in glutathione reductase from chloroquine-sensitive *Plasmodium falciparum* 3D7, *Mol. Biochem. Parasitol. 107*, 169−179.
59. Baldwin, J., Farajallah, A. M., Malmquist, N. A., Rathod, P. K., and Phillips, M. A. (2002) Malarial dihydroorotate dehydrogenase: Substrate and inhibitor specificity, *J. Biol. Chem. 277*, 41827−41834.
60. Clarke, J. L., Sodeinde, O., and Mason, P. J. (2003) A unique insertion in *Plasmodium berghei* glucose-6-phosphate dehydrogenase-6-phosphogluconolactonase: Evolutionary and functional studies, *Mol. Biochem. Parasitol. 127*, 1−8.
61. Miller, B. G., Snider, M. J., Wolfenden, R., and Short, S. A. (2001) Dissecting a charged network at the active site of orotidine-5′-phosphate decarboxylase. *J. Biol. Chem. 276*, 15174−15176.
62. Menz, R.I., Cinquin, O., and Christopherson, R. I. (2002) The identification, cloning and functional expression of the gene encoding orotidine 5′-monophosphate (OMP) decarboxylase from *Plasmodium falciparum*, *Ann. Trop. Med. Parasitol. 96*, 469−476.
63. Smiley, J. A., Paneth, P., O'Leary, M. H., Bell, J. B., and Jones, M. E. (1991) Investigation of the enzymatic mechanism of yeast orotidine 5′-monophosphate decarboxylase using ^{13}C kinetic isotope effects, *Biochemistry 30*, 6216−6223.
64. Porter, D. J. T., and Short, S. A. (2000) Yeast orotidine 5′-phosphate decarboxylase: Steady-state and pre-steady-state analysis of the kinetic mechanism of substrate decarboxylation, *Biochemistry 39*, 11788−11800.
65. Miller, B. G., Smiley, J. A., Short, S. A., and Wolfenden, R. (1999) Activity of yeast orotidine 5′-monophosphate decarboxylase in the absence of metals, *J. Biol. Chem. 274*, 23841−23843.
66. Han, B. D., Livingstone, L. R., Pasek, D. A., Yablonski, M. J., and Jones, M. E. (1995) Human uridine monophosphate synthase: Baculovirus expression, immunoaffinity column purification and characterization of the acetylated amino terminus, *Biochemistry 34*, 10835−10843.
67. Traut, T. W., and Temple, B. R. S. (2000) The chemistry of the reaction determines the in variant amino acids during the evolution and divergence of orotidine 5′-monophosphate decarboxylase, *J. Biol. Chem. 275*, 28675−28681.
68. Miller, B. G., Traut, T. W., and Wolfenden, R. (1998) Effects of substrate binding determinants in the transition state for orotidine 5′-monophosphate decarboxylase, *Bioorg. Chem. 26*, 283−288.
69. Miller, B. G., Snider, M. J., Short, S. A., and Wolfenden, R. (2000) Contribution of enzyme-phosphoribosyl contacts to catalysis by orotidine 5′-monophosphate decarboxylase, *Biochemistry 39*, 8113−8118.
70. Miller, B. G., and Wolfenden, R. (2002) Catalytic proficiency: The unusual case of OMP decarboxylase, *Annu. Rev. Biochem. 71*, 847−885.
71. Smiley, J. A., Hay, K. M., and Levison, B. S. (2001) A reexamination of the substrate utilization of 2-thioorotidine 5′-monophosphate by yeast orotidine 5′-monophosphate decarboxylase, *Bioorg. Chem. 29*, 96−106.

BI048439H